

Life Prediction and crack propagation analysis for the Pipe weld Straight component (PWSC) of power plant

Shrikrishna Dhakad¹, Dr.Sanjeev Saxena² Dr.Geeta Agnihotri³

¹SAT I (deg.), college, Vidisha (M.P.), 464001,sk27_dhakad@yahoo.com

²Advanced Materials and Processes Research Institute (AMPRI), Bhopal- 462 026. san_bpl@yahoo.com

³MANIT, Bhopal , professor in the mechanical Engg. Deptt. agnihotrig@manit.ac.in

Abstract:

In the present paper the fatigue crack growth behavior of surface cracked piping component are performed on the basis of the linear elastic fracture mechanics (LEFM) principles with particular interest in its ability and accuracy to predict full scale component tested experimental data. The crack propagation is considered in semi elliptical shape. In the present paper three different diameter Pipe weld straight components (PWSC 12-6, PWSC 16-4, PWSC 16-5) are selected. The two SIF solution (ASM and Bergman) available in the literature, the extreme point SIFs (depth and surface) are determined at initial crack depth of 3.6 mm the case PWSC12-6. The yield strength for the material is 325MPa. In this case, the applied nominal 183MPa stress range, which is 0.56 times the strength of the material. Therefore, for the particular case the plastic zone correction is applied. The two extreme points SIFs are determined at physical crack depth and also at effective crack length. The details of crack depths at which these SIFs are determined are given in Table 1 and Table 2 Corresponding crack lengths determined are also given in these tables. The analysis are also done for remain two pipe , having the different yield strength of the materials. The details of crack

depths at which these SIFs are determined are given in Table 3&4 and Table 5&6 Corresponding crack lengths determined are also given in these tables.

Key-words: Fatigue; Paris equation; Stress intensity factor solution; Crack growth behavior; Power plant component

Introduction:

The present work has been carried out to assess the prediction accuracy of crack growth behavior of experimentally tested full-scale pipe component having outer surface crack in circumferential direction. In case of the studied pipes, two stress intensity factor (SIF) solutions are available in the literature. One is given in

ASM Handbook Vol. 19 [1] appendices based on Mettu SR et al. numerical work and other one proposed by Bergman [2] based on 3D FEM solution using ABAQUS code. These SIF solutions are for semi-elliptical crack profile. In the experimental pipe specimens the initial crack geometry is having a constant depth.. As the SIF solutions for constant depth crack profile are not available in the open literature. In the present work the SIF solutions available in the literature (ASM handbook [1] and Bergman solution [2]) are evaluated to predict the component behaviour using the fracture specimen tested data. Though, the crack profile in the two available SIFs solutions [1, 2] are different than that of experimental study specimen's crack profile, these have been used to understand the effect of assumed crack profile in the predicted results. The present study have been done on material used in Indian nuclear power plant component.

2. Experimental tested data

2.1 Material properties

The tensile properties of SA333Gr.6 carbon steel base material tested at room temperature have been considered in the present study. The material Young's modulus is 203Gpa and the Yield strength is 302MPa, ultimate tensile strength is 450MPa & Poisson's ratio 0.3. The fatigue crack growth tests were reported [3] to be conducted on the standard three point bend fracture specimen. The material constants of Paris crack growth law had been evaluated by fitting the test data points that is giving in the form of equation below as shown in Table 2.1. Table 2.2 showed the material fatigue data for base and weld metal for the material studied. Table 2.1 Tensile properties of SA333Gr.6 carbon steel tested at room temperature

Material	Yield strength σ_Y (MPa)	Ultimate tensile strength (MPa)	Elongation (%)	% reduction in area	E(GPa)	μ
Base	302	450	36.7	72.96	203	0.3
Weld	325	466	18.7	-	203	0.3

Table 2.2 Paris constant values for the material studied

Pipe case	Stress ratio	Notch location	Paris constant	
			C (mm)	M
406mm pipe	0.1	Base	8.87×10^{-10}	3.80
219mm pipe	0.1	Base	3.807×10^{-9}	3.034
406mm pipe	0.5	Weld	6.98×10^{-10}	3.650
219mm pipe	0.5	Weld	4.279×10^{-9}	2.90397

2.3 Pipe specimen test data

In the present study, three different outer diameter pipes having 219 mm, 324mm and 406 mm used in the piping system of Indian PHWRs have been used for test. The pipe specimens have surface notches of different sizes machined at the outer surface in the circumferential direction by a milling machining process. The experimental data gathered from the literature for the present study are shown in Table 2.3

$$\frac{da}{dN} = 3.807 \times 10^{-9} (\Delta K)^{3.03445} \quad (1)$$

for stress ratio (R) = 0.1

Here da/dN is in m/cycle and ΔK is in $\text{MPa}\sqrt{\text{m}}$.

The full-scale pipe used in the primary heat transporting system of Indian nuclear power plant has been taken in the present study [4].

Methodology used:

With the use of crack growth laws it is possible to predict the life of the piping component subjected to fatigue. For a structure under fluctuating loads, the crack growth rate can be related to the variation of SIF, ΔK , during a load cycle. ΔK has considerable influence on fatigue crack growth and if ΔK remains constant, the crack growth rate is also constant. Paris has expressed the relationship between crack growth

rate (da/dN) and ΔK as a power law in the following form:

$$\frac{da}{dN} = C(\Delta K)^m \quad (2)$$

Where C and m are crack growth constants and $\Delta K = K_{max} - K_{min}$. The quantities K_{max} and K_{min} are the SIF values corresponding to the maximum and minimum stress levels in the fatigue load cycles. For the assumed initial crack depth, the number of cycles required for the incremental increase in crack depth can be calculated as follows from Eqn.(3)

$$dN = \frac{da}{C(\Delta K_d)^m} \quad (3)$$

ΔK_d - SIF range at deepest point of surface crack

$$dc = dN \times C(\Delta K_c)^m \quad (4)$$

where dc - Extension of crack length and ΔK_c - SIF range at surface crack tip. The computation of crack propagation along the two directions has to be carried out simultaneously since Eqns.(3) &(4) are not independent. Now the new dimensions of the crack are calculated as:

$$a_{new} = a_{old} + da \quad (5)$$

$$2c_{new} = 2c_{old} + dc \quad (6)$$

The process is repeated until the crack reaches through-thickness or K reaches fracture toughness of the material. For every incremental increase in crack depth, the life cycles are calculated using Eqn.(3) and added up-to through-thickness, to give the total life of the piping component corresponding to through-thickness crack.(LEFM).SIF is measure if the stress surrounding the crack tip of a body and is

$$K = f \times \sigma_b \times (\pi a)^{0.5} \quad (7)$$

Where f is the function that depend on the geometry of the crack and cracked part under consideration. A is the crack size and σ_b is the nominal stress action normal to the crack. The geometry factor f find from ASM E - 647 and data book with the help of experimental tested solution available different problem. By calculating the SIF, the process of crack growth can be determined. If the SIF is lower than the threshold value no crack propagation is expected.

The SIF excesses the upper material value K_c called fracture toughness the crack propagation is unstable with cause failure of the components. In the range between these two limits stable crack grow can be observed. If the value of bending stress (σ_b) is more then 30 to 40 % yield strength of material (σ_y).

$$a_{eff} = a + 1/3 \pi (k_d / \sigma_y)^2 \quad (8)$$

$$2_{ceff} = 2c + 2/3 \pi (\sqrt{k_s / \sigma_y})^2 \quad (9)$$

da – Assumed increase in crack depth.

Then the extension of crack length at the surface can be calculated by putting the number of cycles obtained from Eqn.(4) to the following equation:

Using two SIF solutions the extreme point SIFs are calculated at initial crack geometry (initial crack length) in mm, crack depths and new lengths are calculated for each increase in crack depth. The process is repeated until the crack reaches through-thickness. prediction results using ASM & M-Bargman solution for (PWSC 12-6, PWSC 16-4, & PWSC 16-5) are shown in Tables 4.1 & 4.2 for the PWSC 12-6.

4. Result and discussion

Using the methodology described in chapter -3 and two SIF solution (ASM and Bergman) available in the literature, the extreme point SIFs (depth and surface) are determined at initial crack depth of 3.6mm the case PWSC12-6. The yield strength for the material is 325MPa. In this case, the applied nominal 183MPa stress range, which is 0.56 times the strength of the material. Therefore, for the particular case the plastic zone correction is applied. The two extreme points SIFs are determined at physical crack depth and also at effective crack length. The details of crack depths at which these SIFs are determined are given in Table 4.1 and Table 4.2. Corresponding crack lengths determined are also given in these tables. The determined SIF range for the case is found lesser than the fracture toughness of the material. Therefore, using Paris equation, the crack growth prediction process is repeated up-to through-wall crack depth.

Fig.1 showed the variation of SIF solution with crack depth predicted by two SIF solution considered in the present study. The depth position SIF values SIF values predicted by Bergman solution compares well with that by ASM solution. Similarly, the surface position SIF predicted by Bergman SIF solution compares well initially with ASM handbook SIF solution thereafter Bergman solution gives higher predicted value of SIF as compared to ASM predicted value. Fig.2 showed the comparison of predicted crack growth behaviour with experimental results, Fig. 3 Variation of crack length with fatigue cycles, Fig. 4 Variation of aspect ratio with fatigue cycles & Fig. 5 Variation of aspect ratio with crack depth

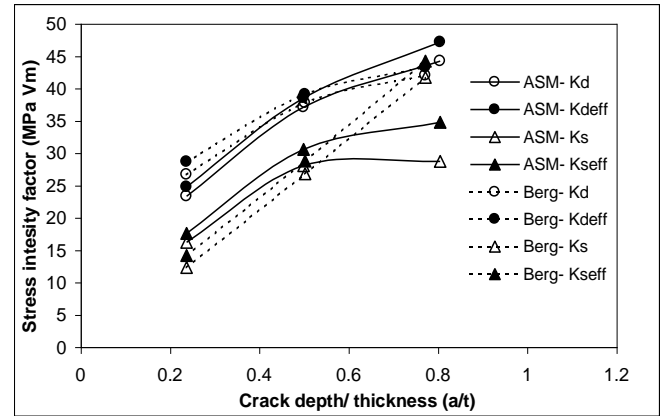


Fig. 1 Variation of SIF range with crack depth for pipe case PWSC12-6

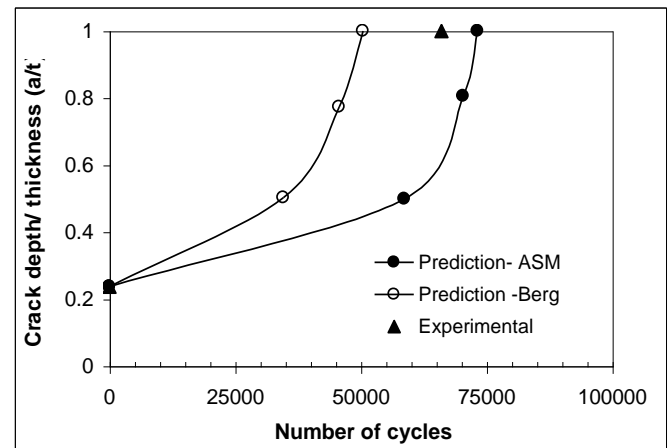


Fig. 2 Variation of a/t with fatigue cycles for pipe case PWSC12-6

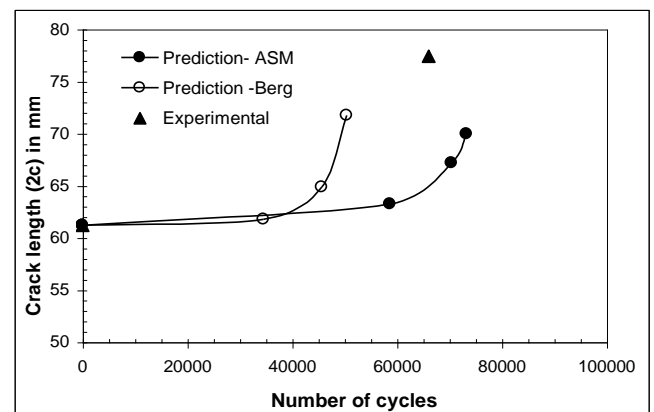


Fig. 3 Variation of crack length with fatigue cycles for pipe case PWSC12-6

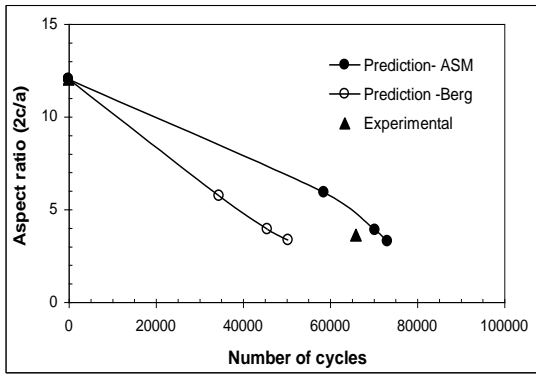


Fig. 4 Variation of aspect ratio with fatigue cycles for pipe case PWSC12-6

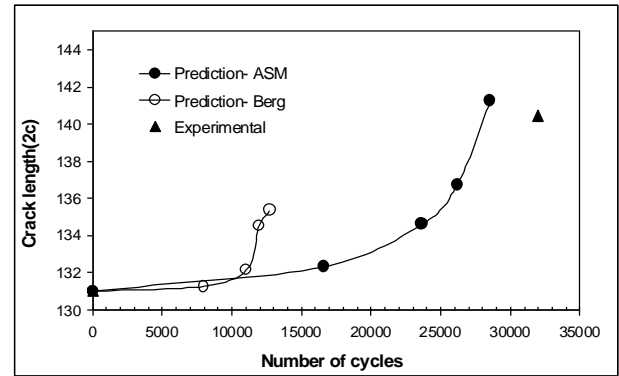


Fig. 8 Variation of crack length with fatigue cycles

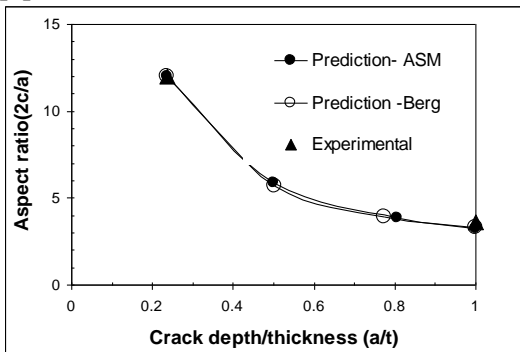


Fig. 5 Variation of aspect ratio with crack depth for pipe case PWSC12-6 case PWSC 16-4

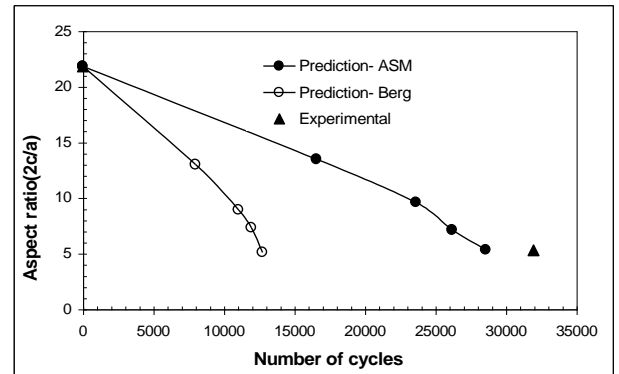


Fig. 9 Variation of aspect ratio with fatigue cycles

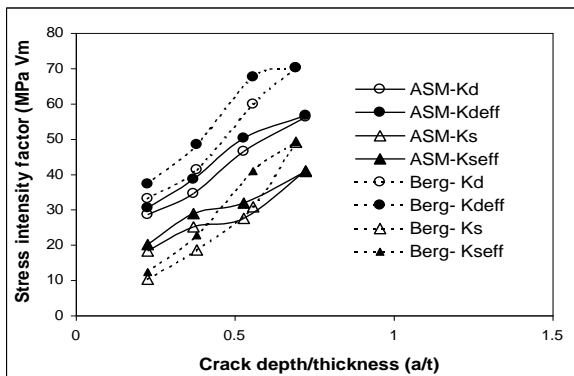


Fig. 6 Variation of SIF range with crack depth

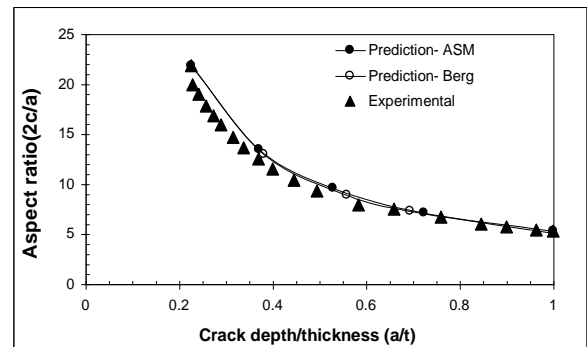


Fig. 10 Variation of aspect ratio with crack depth case PWSC 16-5

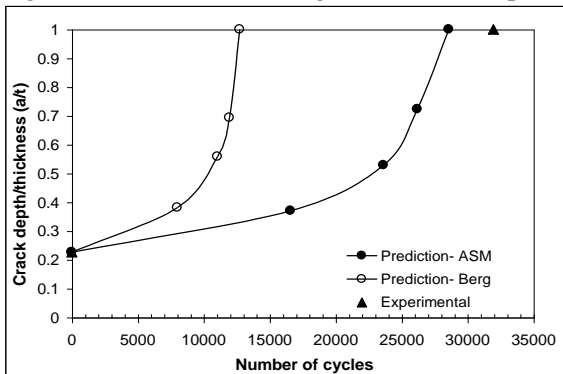


Fig. 7 Variation of crack depth/ thickness with fatigue cycles

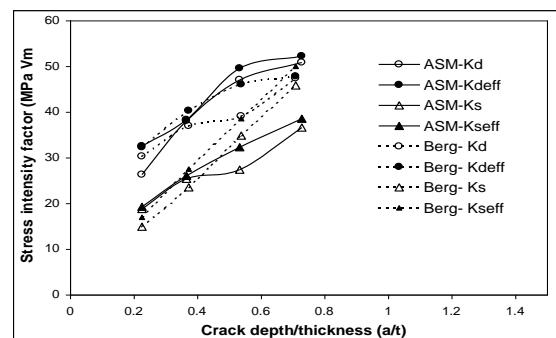


Fig. 11 Variation of SIF range with crack depth

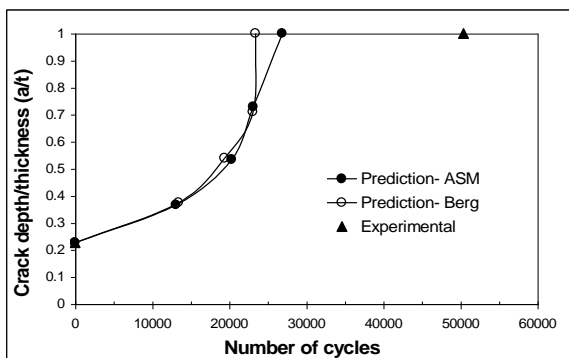


Fig. 12 Variation of crack depth/ thickness with fatigue cycles

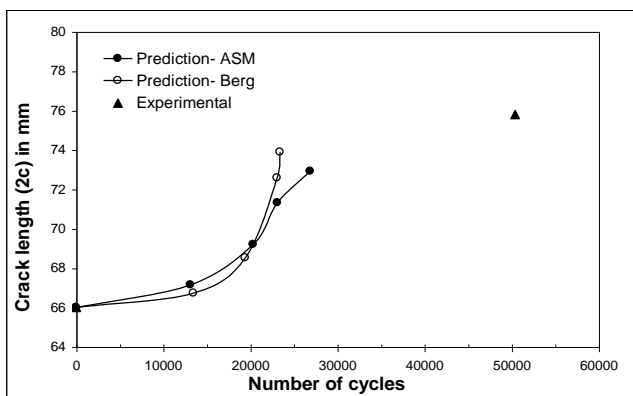


Fig. 13 Variation of crack length with fatigue cycles

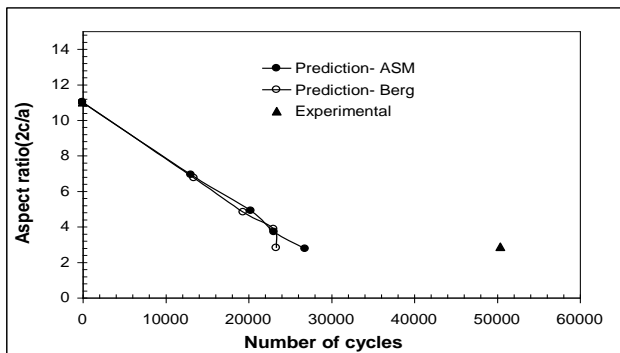


Fig. 14 Variation of aspect ratio with fatigue cycles

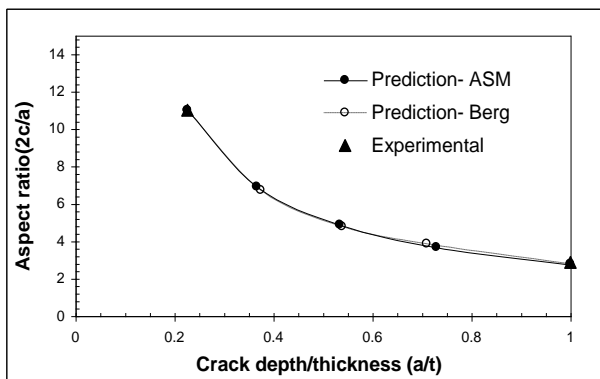


Fig. 15 Variation of aspect ratio with crack depth

Pipe case	Exp.	Prediction method		% error	
		ASM	Bergman	ASM	Bergman
PWSC 12-6	77.4	69.95	71.73	+9.6%	+7.3%
PWSC 16-4	5	0	73.89	+0.25%	+4.44%
PWSC-16-5	75.79	74.3		+1.96%	+2.50%

Note: + tive sign Under prediction; - tive sign Over prediction

5. Conclusion:

It can be observed in the present study results that the initial crack size, aspect ratio of crack, applied bending stress range, stress ratio, diameter of the pipe are some of the factors affecting the fatigue crack growth life of the piping component. For the material studied in the present case and comparing the results of base and weld metal fatigue crack growth behaviour, it can be concluded that the two fatigue crack growth behaviour compares well.

Reference:

- [1] ASM Handbook Vol. 19. Fatigue and Fracture. ASM international, the material information society, 1996; Appendices: 980-1000.
- [2] Bergman M. "Stress intensity factors for circumferential surface cracks in pipes" Int. Frac. Engg Mat. Struct., vol. 18, no. 10(1995)1155-1172.
- [3] Singh PK, Vaze KK, Bhasin V, Kushwaha HS, Ghandhi P, Ramachandra Murthy DS, "Crack initiation and growth behaviour of circumferentially cracked pipes under cyclic and monotonic loading", Int. Jr. of Pres. Ves. and Piping vol. 80, 2003, pp 629- 640.
- [4] Singh PK, Bhasin V, Vaze KK, Ghosh AK, Kushwaha, RamachandraMurthy DS, Gandhi P and Sivaprasad S. Fatigue studies on carbon steel piping materials and components: Indian PHWRs. Nucl. Engg. Design. 238 (2008) 801-813.
- [5] Andersson P, Bergman M, Bricks B, Dahlberg L, Nilsson F, Sattari-Far I. A procedure for safety assessment of components with cracks-handbook. SAQ/FoU Report 96/08. Stockholm: SAQ Kontrol Lab. 1998.
- [6] Soni RS, Kushwaha HS, Mahajan SC, Kakodkar A. Qualification of PHT integrated piping system of 500 MWe PHWR Technical report BARC/1998/E/006.
- [7] E606-93, Standard test method for measurement of fatigue crack growth rate. Annual book of ASTM standard, vol. 03.01;1995.

Comparison of final crack length

Table - 2.3 Details of the experimental results of surface cracked pip

S.No.	Notch location	OD mm	t mm	Outer Span mm	Inner span mm	Load (KN)		Stress range (MPa)	Crack Length (2c) mm	Through wall crack cycles
						Max	Min.			
PWS C12-6	Weld metal	324	21.5	5000	1480	320	32	183	61.2	66000
PWS C 16-4	Weld metal	406	26.5	6500	1600	500	50	196	131	31950
PWS C 16-5	Weld metal	406	26.5	6500	1600	500	50	196	66	50400

Table 4.2 Predicted results using Bergman

a (mm)	2c (mm)	a _{eff} (mm)	2 c _{eff} (mm)	a _{eff} /t	2 c _{eff} / a _{eff}	K _s MPa √m	K _d MPa √m	K _{s(eff)} MPa √m	K _{d(eff)} MPa √m	dN
5.1	61.2	5.73	61.809	0.2665	10.786	16.18	23.27	17.54	24.754	
10.73	63.229	12.32	65.05	0.513	5.31	28.04	37.06	30.554	38.48	58655
17.32	67.2	19.5936	69.012	0.9113	3.522	28.67	44.22	34.75	47.135	11722
21.5	69.9594			1						2864
a (mm)	2c (mm)	a _{eff} (mm)	2 c _{eff} (mm)	a _{eff} /t	2 c _{eff} / a _{eff}	K _s MPa √m	K _d MPa √m	K _{s(eff)} MPa √m	K _{d(eff)} MPa √m	dN
5.1	61.2	5.81	61.505	0.27	10.581	12.3	26.63	14.112	28.618	
10.8	61.78	11.61	63.226	0.54019	5.4438	26.78	37.75	28.73	39.06	34544
16.6	64.84	18.38	68.385	0.85	3.72	41.69	41.95	44.2	43.23	11099
21.5	71.73			1						4782